An Original Study

Hip Osseous Morphology Using Computer Navigation and Plain Radiographs

Rachel M. Frank, MD, Jeremy Alland, BS, Robert C. Grumet, MD, Mark A. Slabaugh, MD, James M. Williams, PhD, Vincent M. Wang, PhD, Alejandro A. Espinoza Orias, PhD, Bernard R. Bach, Jr, MD, and Shane J. Nho, MD, MS

Abstract

In this study, we used 3-dimensional analysis to comprehensively map the osseous morphology of the acetabulum. Human cadaveric specimens were dissected to the joint capsule for computer navigation analysis. Data points outlining acetabular anatomy—determined using optical sensors—were translated into graphical environments. A clock face template was laid over the transverse plane to determine the projections of acetabular arcs onto the transverse plane. A custom-written software program was used to compute the resulting surface area and was applied to the acetabular articular surface and the fossa. Two independent observers performed all measurements.

Sixteen hips were included. Lateral center edge angle was 36.2° and femoral neck shaft angle was 131°. Mean arc lengths of the acetabular fossa from 3 o'clock (anterior) to 9 o'clock (posterior) were 26, 28, 28, 30, 29, 28, and 27 mm at 3, 2, 1, 12, 11, 10, and 9 o'clock, respectively.

The smallest aspect of the acetabulum is the anterior aspect, and the largest is the superior (12 o'clock); the size increases progressively from anterior to superior. In most cases, the superior arc length, or sourcil, corresponds to the 2 o'clock position, and thus the lateral center edge angle may not necessarily correspond to the lateral aspect of the acetabulum.

After femoroacetabular impingement (FAI) was recognized as an etiology of hip osteoarthritis,[1-6] interest in hip joint preservation surgery increased.[7-12] There is a wide variation in hip osseous morphology (Table I), which can develop into cam and/or pincer FAI. With FAI increasingly being recognized as a hip damage mechanism, particularly in young, active patient populations, nonarthroplasty management options are gaining favor.

Current nonarthroplasty options include nonoperative approaches,[13-15] minimally invasive hip arthroscopy,[4,6,9-12,16-29] open surgical dislocation,[4,23,30-41] periacetabular osteotomy,[42] and total hip arthroplasty (THA). Open surgical hip dislocation, traditionally considered the gold standard for FAI, has had good to excellent, technically reproducible results.[40,41] Although this technique provides excellent visualization and typically allows for muscle preservation, its open nature exposes patients to an amount of morbidity not seen with less invasive techniques, including arthroscopically-assisted and all-arthroscopic procedures.

The normal morphologic characteristics of the acetabular joint are poorly understood, and there remains a paucity of basic studies that adequately describe normal hip osseous morphology. Previous studies[43-45] have described the morphology of the hip joint but have been limited in their methodology and clinical applicability. Other studies have analyzed computed tomography (CT)–based computer navigation models to describe hip anatomy, but the results of these studies have been discouraging[46] or not clinically relevant.[47] One of the major challenges in surgical management of FAI is the inability to determine the precise anatomical location and severity of the impingement.

Understanding 3-dimensional (3-D) hip anatomy

Table I. Etiologies of Abnormal Hip Osseous Morphology

Acetabular	Femoral
Retroversion	Coxa vara
Coxa profunda	Slipped capital femoral epiphysis
Coxa protrusio	Femoral head avascular necrosis
Dysplasia	Posttraumatic, iatrogenic
Posttraumatic, iatrogenic	Retrotorsion
	Legg-Calvé-Perthes disease

Dr. Frank is Resident, Department of Orthopaedic Surgery, Mr. Alland is Medical Student, Dr. Grumet is Attending Orthopaedic Surgeon, Department of Orthopaedic Surgery, Dr. Slabaugh is Attending Orthopaedic Surgeon, Department of Orthopaedic Surgery, Dr. Williams is Professor, Department of Anatomy and Cell Biology, Biochemistry, Internal Medicine, Dr. Wang is Assistant Professor, Department of Orthopaedic Surgery, Dr. Espinoza is Instructor Assistant Director, Department of Orthopaedic Surgery, Dr. Bach is Attending Orthopaedic Surgeon, Department of Orthopaedic Surgery, and Dr. Nho is Attending Orthopaedic Surgeon, Department of Orthopaedic Surgery, Division of Sports Medicine, Department of Orthopaedic Surgery, Rush University Medical Center, Chicago, Illinois.

Address correspondence to: Rachel M. Frank, MD, Department of Orthopaedic Surgery, Rush University Medical Center, 1611 W Harrison St, Suite 300, Chicago, IL 60612 (tel, 312-243-4244; fax, 708-492-5525; e-mail, rmfrank3@gmail.com).

Am J Orthop. 2012;41(11):519-525.

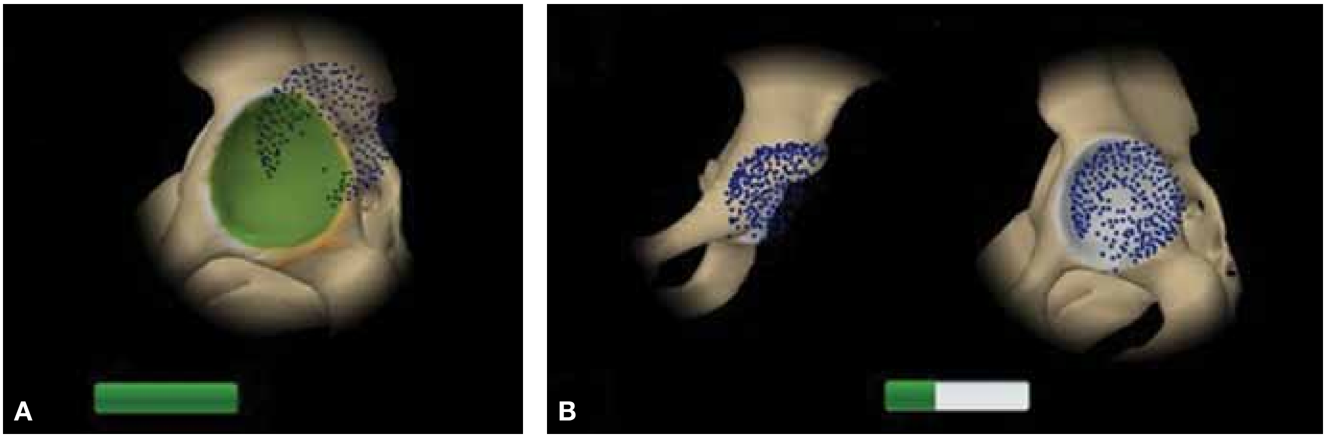

Figure 1. In these screen shots produced with hip arthroplasty software (BrainLAB, Feldkirchen, Germany), (A) point cloud represents surface area of acetabulum, and (B) fossa and acetabulum points are used to reconstruct hip morphology in 3 dimensions.

allows orthopedic surgeons to plan appropriate hip joint preservation surgery. In the study, we used 3-D analysis to comprehensively map the osseous morphology of the acetabulum. We also correlated the 3-D anatomical data to standard radiographic images to further enhance preoperative planning. We hypothesized that our acetabular osseous anatomical findings, as determined with radiograph and computer-based 3-D analysis, would be consistent with those reported in the literature and that the acetabulum would be largest at its superior-most aspect.

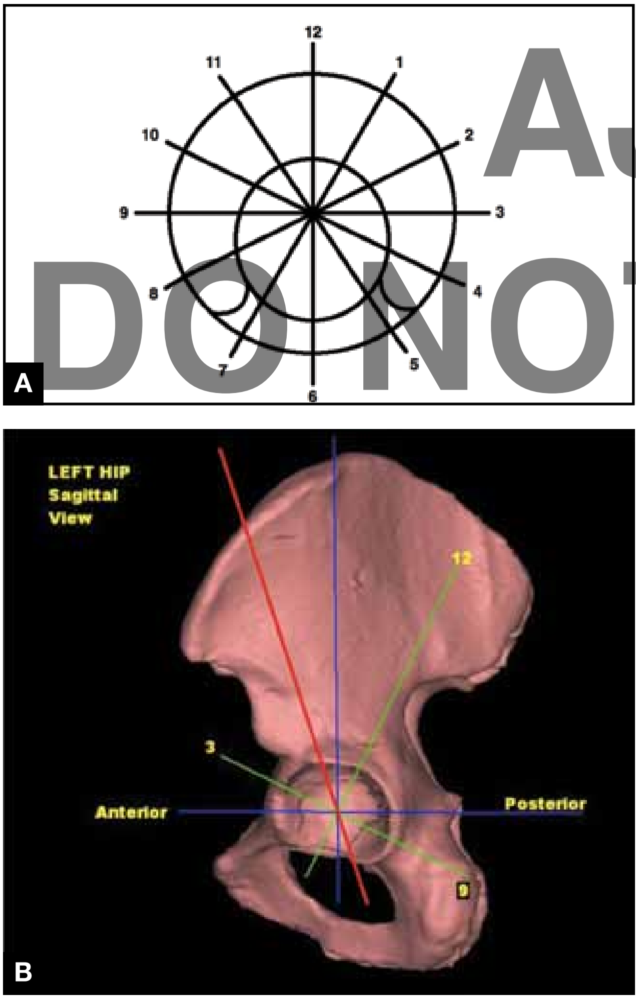

Figure 2. (A) Clock face applied to acetabular surface. Each time on clock represents measured arc length. (B) Clock face applied to 3-D acetabular morphology. For left hip, 3 o'clock direction corresponds to anterior of joint, and 9 o'clock direction corresponds to posterior of joint.

Materials and Methods

Thirty-six human cadaveric specimens (72 hips) were available for analysis. A standard anteroposterior plain radiograph was taken of each pelvis with the cadaver in a supine position. All radiographs were obtained with the coccyx positioned in the midline, approximately 1 cm above the pubic symphysis (neutral tilt); the obturator foramen and the greater trochanter were symmetrical (neutral rotation). After the radiographs were reviewed, only those hips from baseline healthy donors, Tönnis scale[48] grade 0 (no osteoarthritis) or grade 1 (increased sclerosis at head and/or acetabulum, slight narrowing of joint space, moderate loss of sphericity of head) were used in the 3-D morphologic analysis. Hips with Tönnis scale grade 2 (small cysts in head/or acetabulum, increased narrowing of joint space, moderate loss of sphericity of head) or grade 3 (large cysts in head and/or acetabulum, severe narrowing or obliteration of joint space, severe deformity of the head) were excluded from further analysis.

A sports medicine fellowship–trained orthopedic surgeon used tools in our Picture Archiving and Communication System to grade all radiographs. Joint space was measured at 2 points (lateral, medial), and several parameters[49] were considered (Tönnis angle, Sharp angle, lateral center edge [LCE] angle of Wiberg, femoral neck shaft [FNS] angle, crossover sign, posterior wall sign).

Hips that met the study criteria were dissected to the level of the hip joint capsule without removing cartilage from the acetabulum. A computer navigation system, Hip Resurfacing Application (BrainLAB, Feldkirchen, Germany), was then used to acquire the geometry of the eligible hips. Optical sensors were placed in appropriate bony landmarks, including the anterior superior iliac spine and the proximal femur, according to manufacturer specifications. The navigation system's THA software was used to place the optical pointer in the deepest point of the acetabular fossa, and 50 data points were obtained. Similarly, with use of the optical pointer, 200 data points were obtained from the acetabular articular surface, by outlining the borders of the articular surface and then drawing circumferential and radial lines (Figure 1).

The point cloud data acquired with the navigation system were translated into a graphical computer-aided design environment (SolidWorks 2007; Dassault Systèmes SolidWorks Corp, Waltham, Massachusetts). Orthogonal datum planes (equivalent to transverse, sagittal, and coronal planes) were created as a local coordinate system centered at the acetabular/femoral centroids, as determined by the navigation system. Radial lengths and acetabular depth were thus measured. A clock face template was applied to the transverse plane to determine the 3 o'clock (anterior) through 9 o'clock (posterior) positions and projections of the arcs onto the transverse plane (Figure 2).

A Visual C++ program custom-written under the Microsoft Foundation Class programming environment was used to produce a mesh from the point cloud data and compute the resulting surface area. This program was applied to the acetabular articular surface and to the fossa (Figure 3).

Radiographs of the hip specimens were correlated to the 3-D data. Applying ImageJ software (National Institutes of Health [NIH], Bethesda, Maryland) to the radiographs, 2 independent observers measured arc length from the center of the hip joint to the superior edge of the acetabulum (Figure 4). This arc length was then compared to the arc length from the correlating hip specimen collected during 3-D analysis. The clock face value with the 3-D analysis arc length closest to the radiograph arc length was recorded. The mode of the clock face values was used to correlate the radiographs to the 3-D models. All the data were used to make anatomical recreations of the acetabular morphology (Figure 5).

Outcomes of interest from the radiographic measurements included lateral joint space width, medial joint space width, LCE angle, and FNS angle. Outcomes of interest computed from the acetabular 3-D mesh included surface area, radius, and depth of acetabular articular surface and fossa. In addition, arc lengths by clock face positions were measured.

For the nondescriptive components of this anatomical study, statistical analysis for the calculation of interobserver and intraobserver reliability was performed with the intraclass correlation coefficient. A correlation matrix and individual Pearson correlation coefficients were used to compare navigation system arc lengths and radiograph arc lengths. All statistical analyses were conducted with statistical software (SPSS, Chicago, Illinois), and results were considered significant at $P<.05$.

Results

Sixteen specimens met the study criteria. Mean (SD) age was 73 (12) years. As measured on plain radiographs, mean (SD) joint space was 6.2 (1.0) mm laterally and 4.9 (1.1) mm medially. In addition, mean (SD) LCE angle was 36.2° (5.4º), and mean (SD) FNS angle was 130.9° (3.7º). The data were manipulated for right and left hips to ensure that 3 o'clock represented the anterior of the hip and 9 o'clock represented the posterior of the hip.

The acetabular mesh was used to compute surface area, radius, and depth and was applied to the acetabular articular surface as well as the fossa. Mean (SD) surface area of the acetabular fossa was 474.1 (72.1) mm^2, and mean surface area of the articular surface was 2642.5 (536.9) mm^2. Mean (SD) radius was 23.3 (1.7) mm, and mean (SD) depth was 27.9 (2.6) mm. The largest arc lengths were in the 12 o'clock direction; arc lengths decreased both clockwise and counterclockwise from 12 o'clock. Mean arc lengths for each clock direction and mean radial measurements of the acetabular articular surface are described in Table II and Figure 6.

For each arc length measured with ImageJ (NIH) software, intraobserver reliability and interobserver reliability were high. Intraclass correlation coefficient was

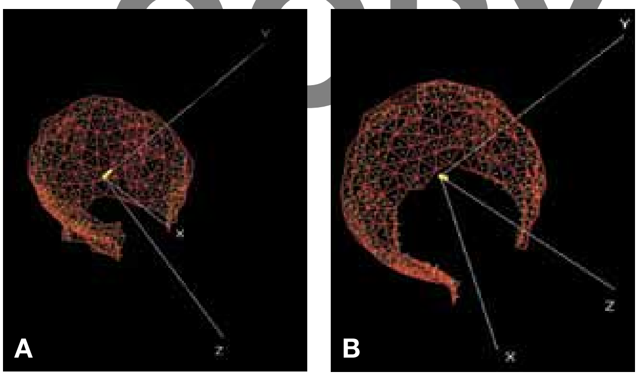

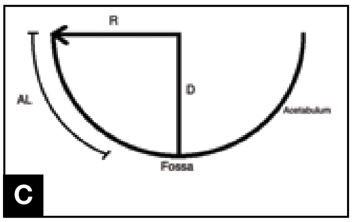

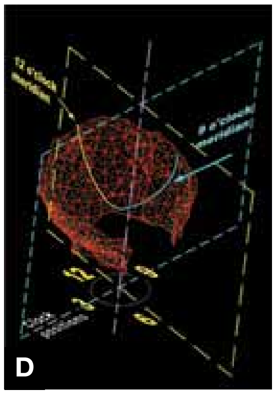

Figure 3. (A, B) Two views of acetabular articular surface mesh. Visual C++ program custom-written under Microsoft Foundation Class programming environment was used to produce mesh images. (C) Acetabulum and fossa with measurement variables assigned (R, radius; D, depth; AL, arc length). (D) Modified 3-dimensional mesh depicts clock face "meridians."

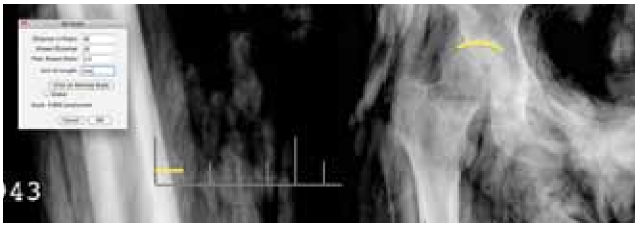

Figure 4. Hip specimen radiographs correlated to 3-D data. ImageJ software (National Institutes of Health, Bethesda, Maryland) was used on radiographs to measure arc length from center of hip joint to superior edge of acetabulum. Radiograph values were compared with 3-D analysis values for same hip specimen.

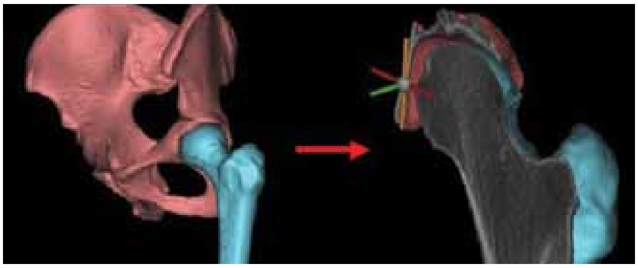

Figure 5. 3-D hip morphology reconstructions from patient-based computed tomography scans will be used to measure arc lengths and acetabular/femoral version.

.995 ($P<.001$) within each observer and between observers. Furthermore, radiograph arc lengths and navigation system arc lengths correlated highly ($R = 0.274$) at the 2 o'clock position.

Discussion

The 4 principal findings of this study are:

- The largest distance from the acetabular fossa to the outer edge of the acetabulum is at 12 o'clock.
- Distances from the acetabular fossa progressively decrease in the anterior direction (3 o'clock) and in the posterior direction (9 o'clock).
- The anterior acetabular wall appears to decrease more dramatically at 4 o'clock.
- The acetabular arc length (or sourcil) may correspond to a point between 10 o'clock and 2 o'clock but in most cases corresponds to 2 o'clock, and, thus, the LCE angle may not necessarily correspond to the lateral-most aspect of the acetabulum.

This contributes additional, novel information to the growing body of literature on normal femoroacetabular osseous morphology.

There is no consensus on normal hip osseous anatomy. For example, although the anatomy of the anterior acetabular ridge has been consistently described as irregular, and includes curved, angular, irregular, and straight configurations,[43-45] the posterior acetabular rim has been described as hypoplastic in some studies[50] but not others.[43,51,52] In addition, most of the published morphologic studies were designed to help with the design and sizing of acetabular components for THA. Although the anatomical data presented in these studies[43-45,50,51,53] are clearly relevant, there is still need for a better understanding of normal hip osseous morphology from a minimally invasive, nonarthroplasty perspective.

Surgical intervention may be able to prevent hip osteoarthritis. For example, pincer FAI can be managed by trimming the acetabular rim. Knowledge of the hip morphology is a must when deciding whether a patient is a candidate for an acetabular rim trim. The results of this 3-D analysis of the acetabulum provide more insight into the normal anatomy of the hip joint. As the depth around the circumference of the acetabular surface is not constant, the rim extends a variety of arc lengths. For example, the distance to the anterior rim is smaller than the distance to the posterior rim. In addition, the longest length is at the superior aspect of the acetabular rim. These results set the standard for the normal morphology of the acetabulum, which is required for the diagnosis and ultimately for the management of anatomical abnormalities of insidious onset or resulting from acute injury.

A comprehensive definition of the normal morphology of the hip joint can also be applied to preoperative planning. A hip radiograph provides a clear delineation of arc lengths from the center of the joint to the acetabular rim in 2 dimensions. In this study, the length of the superior arc was compared with the 3-D data

Table II. Arc Lengths From Each Clock Face Direction[a], Compared With Corresponding Arc Lengths of Each Specimen

	Clock Face Direction											
Specimen Arc Length, mm	**7**	**8**	**9**	**10**	**11**	**12**	**1**	**2**	**3**	**4**	**5**	**6**
Mean	20.3	23.03	26.98	27.83	29.27	30.16	28.21	28.41	25.79	20.33	18.34	15.79
Minimum	9.74	11.95	18.42	18.1	21.71	25.34	21.96	21.91	14.87	10.3	16.32	15.79
Maximum	25.7	27.54	42.25	35.94	34.56	39.68	32.97	39.76	44.39	27.67	20.53	15.79
SD	4.67	4.4	6.45	4.65	3.61	3.8	3.12	5.35	7.62	4.59	1.78	N/A

[a]The data were manipulated for right and left hips to ensure that 3 o'clock represented the anterior of the hip and 9 o'clock represented the posterior of the hip.
Abbreviation: N/A, not applicable.

to determine which clock face value correlated best to the 2-dimensional (2-D) arcs. In this comparison, the superior radiographic arc appeared to be represented at the 2 o'clock position in 37% of cases and at 1 o'clock in 19% of cases. The 12 o'clock position corresponded to only 6% of cases, and therefore the LCE angle may not correspond to the largest arc length of the acetabulum. Similarly, when the radiographic measurement of acetabular arc length was statistically compared with the mean 3-D acetabular arc lengths measured at each clock face position, the strongest correlation with the radiographic view was at the 2 o'clock position. Of note, the acetabular version, which was not measured in the present study, may have also affected the relationship between the radiographic acetabular arc length. Surgeons can apply this information by using the noninvasive radiograph to estimate the 3-D anatomy. More studies are needed to further determine the relationship between the 3-D measurements and the 2-D radiographs.

In 2001, Maruyama and colleagues[44] studied the morphologic features of 100 human cadaveric hips, with the goal of analyzing acetabular and femoral anteversion angles as well as femoral head offset. The authors reported 4 distinct anterior acetabular ridge configurations: curved, angular, irregular, and straight. A curved configuration was most commonly found, accounting for 61% of the specimens' morphology. The results from that investigation were supported in 2007 by Vandenbussche and colleagues,[54] who morphologically studied the acetabular rim with the goal of determining a way to prevent iliopsoas impingement after THA. Using 34 human cadaveric pelvises, the authors found the morphology of the acetabular rim to be an asymmetric succession of peaks and valleys and coined the phrase *psoas valley* for the acetabular rim.

Similarly, in 2008, Vandenbussche and colleagues[45] studied the morphologic characteristics of 200 healthy human hips. The authors used CT scans to digitize the acetabular ridge of each hip onto 3-D bone reconstructions, confirmed that the acetabular rim is an asymmetric succession of peaks and troughs, and found the geometry of the psoas valley (anterior ridge) most commonly curved, followed by near equal distributions of irregular and angular. Unlike Maruyama and colleagues,[44] the authors did not find any specimens with a straight configuration.

Kohnlein and colleagues[43] recently examined 66 acetabula from 33 human cadaveric specimens and described their morphologic findings. Mean (SD) age was 44 (15) years. A single observer used plaster molds reconstructed from the bony acetabulum to create a model to be used to perform measurements. In that model, similar to ours, a clock face was used to describe the geometry of the acetabulum. However, whereas we used computer navigation software in our study, Kohnlein and colleagues used a measuring tape and a goniometer to measure acetabular depths and arc lengths by hand.

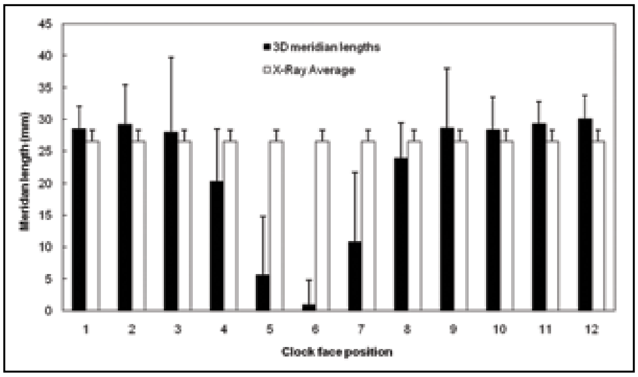

Figure 6. Results of radiograph correlations to clock face arc lengths.

They also studied acetabular inclination, version, and tilt after manually reconstructing the previously separated pelvises; we did not analyze this information. Their finding, similar to ours and to that reported in other studies, is that the acetabular rim has a nonuniform morphology, with peaks and depressions along the rim. Although they focused more on acetabular version, tilt, and inclination, we focused more on surface area, radius, depth, and arc length of the acetabulum, which allows for characterization of the overall acetabular morphology.

The study by Kohnlein and colleagues[43] was well designed but had several limitations: single observer, specimens obtained from a collection dating to the 6th through 13th centuries, and use of plaster molds and hand-based measurements for data collection. Perhaps the most clinically relevant limitation was the lack of cartilage in the hips. In our study, all the measurements were taken by 2 independent observers, providing excellent reliability. In addition, computer-based measurements and 3-D navigation software were used for all data measurements, providing excellent precision and accuracy of the data.

Although they were not examining normal hip osseous morphology, Tannast and colleagues[47] developed, validated, and used a noninvasive, CT-based method to assess FAI. They developed software (HipMotion) to reconstruct a 3-D model of the pelvis and femur from CT scans so that they could anatomically calculate the range of motion of each hip, identify the impingement zone, and simulate postoperative hip motion. They validated their software by comparing their virtual measurements with measurements made with the THA software of BrainLAB.

The results from the study by Tannast and colleagues[47] may represent the future of using noninvasive 3-D models for preoperative planning and intraoperative management of FAI. However, the need for a similar model describing normal hip osseous morphology remains. In 2009, Zumstein and colleagues[55] conducted a cadaveric study of a hip arthroscopy method that, in managing pincer FAI, avoids the posterolateral portal. Each cadaver hip was dissected after the presumed pincer FAI lesion was arthroscopically trimmed, and then the area being managed was analyzed. The authors found their presumed posterior starting point, and thus their planned arc of tissue resection significantly underestimated the actual arc of resection. The authors concluded that accurate preoperative planning for arthroscopic management of pincer FAI is crucial, further highlighting the importance of determining normal acetabular anatomy.

The present study addressed previous limitations by using a computer-based 3-D measurement system. Through use of data points, the BrainLAB system can recreate a 3-D hip model, which provides more accuracy and precision than human-based measurements do. In addition, the present study used multiple observers for data analysis to minimize observer bias and human error. Another strength of this study is its use of recently donated human cadavers with intact cartilage, representing current body types and allowing for full dissection and manipulation. However, the cadaveric specimens were also a limitation, as the population consisted mostly of the elderly and the diseased, obviously not representative of the general population.

In summary, the present study demonstrated that the longest distance from the acetabular fossa to the outer edge of the acetabulum was at 12 o'clock and that distances progressively decrease in both the anterior direction (3 o'clock) and the posterior direction (9 o'clock). Furthermore, the anterior acetabular wall appears to decrease more dramatically at 4 o'clock.

Radiographically, the superior arc length (or sourcil) may correspond to a point between 10 o'clock and 2 o'clock but in most cases corresponds to 2 o'clock, and, thus, the LCE angle may not necessarily correspond to the lateral-most aspect of the acetabulum. Clinically, acetabular arc measurements can be used as intraoperative guides in assessing the amount of rim trimming or acetabular reorientation that is necessary. More studies will be conducted to determine the correlation between 3-D CT measurements and radiographic measurements.

Conclusions

The smallest aspect of the acetabulum is the anterior aspect, and the largest is the superior (12 o'clock); the size increases progressively from anterior to superior. In most cases, the superior arc length (or sourcil) corresponds to the 2 o'clock position, and, thus, the LCE angle may not necessarily correspond to the lateral-most aspect of the acetabulum. Having descriptions of normal hip morphology will improve preoperative planning and postoperative outcomes of hip joint preservation surgery.

Authors' Disclosure Statement

The authors report no actual or potential conflict of interest in relation to this article.

References

1. Ganz R, Leunig M, Leunig-Ganz K, Harris WH. The etiology of osteoarthritis of the hip: an integrated mechanical concept. *Clin Orthop*. 2008;466(2):264-272.
2. Ganz R, Parvizi J, Beck M, Leunig M, Notzli H, Siebenrock KA. Femoroacetabular impingement: a cause for osteoarthritis of the hip. *Clin Orthop*. 2003;(417):112-120.
3. Allen D, Beaule PE, Ramadan O, Doucette S. Prevalence of associated deformities and hip pain in patients with cam-type femoroacetabular impingement. *J Bone Joint Surg Br*. 2009;91(5):589-594.
4. Beaule PE, Allen DJ, Clohisy JC, Schoenecker PL, Leunig M. The young adult with hip impingement: deciding on the optimal intervention. *Instr Course Lect*. 2009;58:213-222.
5. Beck M, Kalhor M, Leunig M, Ganz R. Hip morphology influences the pattern of damage to the acetabular cartilage: femoroacetabular impingement as a cause of early osteoarthritis of the hip. *J Bone Joint Surg Br*. 2005;87(7):1012-1018.
6. Parvizi J, Leunig M, Ganz R. Femoroacetabular impingement. *J Am Acad Orthop Surg*. 2007;15(9):561-570.
7. Leunig M, Huff TW, Ganz R. Femoroacetabular impingement: treatment of the acetabular side. *Instr Course Lect*. 2009;58:223-229.
8. Leunig M, Nho SJ, Turchetto L, Ganz R. Protrusio acetabuli: new insights and experience with joint preservation. *Clin Orthop*. 2009;467(9):2241-2250.
9. Byrd JW, Jones KS. Arthroscopic management of femoroacetabular impingement. *Instr Course Lect*. 2009;58:231-239.
10. Murphy S, Tannast M, Kim YJ, Buly R, Millis MB. Debridement of the adult hip for femoroacetabular impingement: indications and preliminary clinical results. *Clin Orthop*. 2004;(429):178-181.
11. Philippon MJ, Stubbs AJ, Schenker ML, Maxwell RB, Ganz R, Leunig M. Arthroscopic management of femoroacetabular impingement: osteoplasty technique and literature review. *Am J Sports Med*. 2007;35(9):1571-1580.
12. Sierra RJ, Trousdale RT, Ganz R, Leunig M. Hip disease in the young, active patient: evaluation and nonarthroplasty surgical options. *J Am Acad Orthop Surg*. 2008;16(12):689-703.
13. Grumet R, Frank R, Slabaugh M, Virkus W, Bush-Joseph C, Nho S. Lateral hip pain in an athletic population: differential diagnosis and treatment options. *Sports Health*. 2010;2(3):191-196.
14. Frank R, Grumet R, Slabaugh M, Virkus W, Bush-Joseph C, Nho S. Posterior hip pain in an athletic population: differential diagnosis and treatment options. *Sports Health*. 2010;2(3):237-246.
15. Keogh MJ, Batt ME. A review of femoroacetabular impingement in athletes. *Sports Med*. 2008;38(10):863-878.
16. Brunner A, Horisberger M, Herzog RF. Sports and recreation activity of patients with femoroacetabular impingement before and after arthroscopic osteoplasty. *Am J Sports Med*. 2009;37(5):917-922.
17. Byrd JW, Jones KS. Prospective analysis of hip arthroscopy with 2-year follow-up. *Arthroscopy*. 2000;16(6):578-587.
18. Gedouin JE, Duperron D, Langlais F, Thomazeau H. Update to femoroacetabular impingement arthroscopic management. *Orthop Traumatol Surg Res*. 2010;96(3):222-227.
19. Horisberger M, Brunner A, Herzog RF. Arthroscopic treatment of femoral acetabular impingement in patients with preoperative generalized degenerative changes. *Arthroscopy*. 2010;26(5):623-629.
20. Ilizaliturri VM Jr, Orozco-Rodriguez L, Acosta-Rodriguez E, Camacho-Galindo J. Arthroscopic treatment of cam-type femoroacetabular impingement: preliminary report at 2 years minimum follow-up. *J Arthroplasty*. 2008;23(2):226-234.
21. Khanduja V, Villar RN. The arthroscopic management of femoroacetabular impingement. *Knee Surg Sports Traumatol Arthrosc*. 2007;15(8):1035-1040.
22. Larson CM, Giveans MR. Arthroscopic management of femoroacetabular impingement: early outcomes measures. *Arthroscopy*. 2008;24(5):540-546.
23. Laude F, Sariali E, Nogier A. Femoroacetabular impingement treatment using arthroscopy and anterior approach. *Clin Orthop*. 2009;467(3):747-752.
24. McCarthy J, Barsoum W, Puri L, Lee JA, Murphy S, Cooke P. The role of hip arthroscopy in the elite athlete. *Clin Orthop*. 2003;(406):71-74.
25. Philippon M, Schenker M, Briggs K, Kuppersmith D. Femoroacetabular impingement in 45 professional athletes: associated pathologies and return to sport following arthroscopic decompression. *Knee Surg Sports Traumatol Arthrosc*. 2007;15(7):908-914.
26. Philippon MJ, Schenker ML. Arthroscopy for the treatment of femoroacetabular impingement in the athlete. *Clin Sports Med*. 2006;25(2):299-308.

27. Philippon MJ, Weiss DR, Kuppersmith DA, Briggs KK, Hay CJ. Arthroscopic labral repair and treatment of femoroacetabular impingement in professional hockey players. *Am J Sports Med*. 2010;38(1):99-104.
28. Philippon MJ, Yen YM, Briggs KK, Kuppersmith DA, Maxwell RB. Early outcomes after hip arthroscopy for femoroacetabular impingement in the athletic adolescent patient: a preliminary report. *J Pediatr Orthop*. 2008;28(7):705-710.
29. Potter BK, Freedman BA, Andersen RC, Bojescul JA, Kuklo TR, Murphy KP. Correlation of Short Form-36 and disability status with outcomes of arthroscopic acetabular labral debridement. *Am J Sports Med*. 2005;33(6):864-870.
30. Anderson LA, Crofoot CD, Erickson J, Morton DA, Peters CL. Acetabular osteochondroplasty and simultaneous reorientation: background and validation of concept. *Orthopedics*. 2010;33(5). doi:10.3928/01477447-20100329-10.
31. Beaule PE, Le Duff MJ, Zaragoza E. Quality of life following femoral head–neck osteochondroplasty for femoroacetabular impingement. *J Bone Joint Surg Am*. 2007;89(4):773-779.
32. Beck M. Groin pain after open FAI surgery: the role of intraarticular adhesions. *Clin Orthop*. 2009;467(3):769-774.
33. Beck M, Leunig M, Parvizi J, Boutier V, Wyss D, Ganz R. Anterior femoroacetabular impingement: part II. Midterm results of surgical treatment. *Clin Orthop*. 2004;(418):67-73.
34. Bizzini M, Notzli HP, Maffiuletti NA. Femoroacetabular impingement in professional ice hockey players: a case series of 5 athletes after open surgical decompression of the hip. *Am J Sports Med*. 2007;35(11):1955-1959.
35. Espinosa N, Rothenfluh DA, Beck M, Ganz R, Leunig M. Treatment of femoro-acetabular impingement: preliminary results of labral refixation. *J Bone Joint Surg Am*. 2006;88(5):925-935.
36. Graves ML, Mast JW. Femoroacetabular impingement: do outcomes reliably improve with surgical dislocations? *Clin Orthop*. 2009;467(3):717-723.
37. Hartmann A, Gunther KP. Arthroscopically assisted anterior decompression for femoroacetabular impingement: technique and early clinical results. *Arch Orthop Trauma Surg*. 2009;129(8):1001-1009.
38. Lincoln M, Johnston K, Muldoon M, Santore R. Combined arthroscopic and modified open approach for cam femoroacetabular impingement: a preliminary experience. *Arthroscopy*. 2009;25(4):392-399.
39. May O, Matar WY, Beaule PE. Treatment of failed arthroscopic acetabular labral debridement by femoral chondro-osteoplasty: a case series of five patients. *J Bone Joint Surg Br*. 2007;89(5):595-598.
40. Peters CL, Erickson JA. Treatment of femoro-acetabular impingement with surgical dislocation and debridement in young adults. *J Bone Joint Surg Am*. 2006;88(8):1735-1741.
41. Peters CL, Schabel K, Anderson L, Erickson J. Open treatment of femoroacetabular impingement is associated with clinical improvement and low complication rate at short-term followup. *Clin Orthop*. 2010;468(2):504-510.
42. Siebenrock KA, Schoeniger R, Ganz R. Anterior femoro-acetabular impingement due to acetabular retroversion. Treatment with periacetabular osteotomy. *J Bone Joint Surg Am*. 2003;85(2):278-286.
43. Kohnlein W, Ganz R, Impellizzeri FM, Leunig M. Acetabular morphology: implications for joint-preserving surgery. *Clin Orthop*. 2009;467(3):682-691.
44. Maruyama M, Feinberg JR, Capello WN, D'Antonio JA. The Frank Stinchfield Award: Morphologic features of the acetabulum and femur: anteversion angle and implant positioning. *Clin Orthop*. 2001;(393):52-65.
45. Vandenbussche E, Saffarini M, Taillieu F, Mutschler C. The asymmetric profile of the acetabulum. *Clin Orthop*. 2008;466(2):417-423.
46. Brunner A, Horisberger M, Herzog RF. Evaluation of a computed tomography–based navigation system prototype for hip arthroscopy in the treatment of femoroacetabular cam impingement. *Arthroscopy*. 2009;25(4):382-391.
47. Tannast M, Kubiak-Langer M, Langlotz F, Puls M, Murphy SB, Siebenrock KA. Noninvasive three-dimensional assessment of femoroacetabular impingement. *J Orthop Res*. 2007;25(1):122-131.
48. Tonnis D, Heinecke A. Acetabular and femoral anteversion: relationship with osteoarthritis of the hip. *J Bone Joint Surg Am*. 1999;81(12):1747-1770.
49. Mast NH, Impellizzeri F, Keller S, Leunig M. Reliability and agreement of measures used in radiographic evaluation of the adult hip. *Clin Orthop*. 2011;469(1):188-199.
50. Giori NJ, Trousdale RT. Acetabular retroversion is associated with osteoarthritis of the hip. *Clin Orthop*. 2003;(417):263-269.
51. Jamali AA, Mladenov K, Meyer DC, et al. Anteroposterior pelvic radiographs to assess acetabular retroversion: high validity of the "cross-over-sign." *J Orthop Res*. 2007;25(6):758-765.
52. Kalberer F, Sierra RJ, Madan SS, Ganz R, Leunig M. Ischial spine projection into the pelvis: a new sign for acetabular retroversion. *Clin Orthop*. 2008;466(3):677-683.
53. Thompson MS, Dawson T, Kuiper JH, Northmore-Ball MD, Tanner KE. Acetabular morphology and resurfacing design. *J Biomech*. 2000;33(12):1645-1653.
54. Vandenbussche E, Saffarini M, Deloge N, Moctezuma JL, Nogler M. Hemispheric cups do not reproduce acetabular rim morphology. *Acta Orthop*. 2007;78(3):327-332.
55. Zumstein M, Hahn F, Sukthankar A, Sussmann PS, Dora C. How accurately can the acetabular rim be trimmed in hip arthroscopy for pincer-type femoral acetabular impingement: a cadaveric investigation. *Arthroscopy*. 2009;25(2):164-168.

This paper will be judged for the Resident Writer's Award.